HUMAN GENE THERAPY 24:306–316 (March 2013)

DOI: 10.1089/hum.2012.104

Stromal Targeting of Sodium Iodide Symporter Using Mesenchymal Stem Cells Allows Enhanced Imaging and Therapy of Hepatocellular Carcinoma

Kerstin Knoop,[1] Nathalie Schwenk,[1] Patrick Dolp,[1] Michael J. Willhauck,[1] Christoph Zischek,[2] Christian Zach,[3] Markus Hacker,[3] Burkhard Göke,[1] Ernst Wagner,[4] Peter J. Nelson,[2] and Christine Spitzweg[1]

Abstract

The tumor-homing property of mesenchymal stem cells (MSC) has lead to their use as delivery vehicles for therapeutic genes. The application of the sodium iodide symporter (NIS) as therapy gene allows noninvasive imaging of functional transgene expression by ^{123}I-scintigraphy or PET-imaging, as well as therapeutic application of ^{131}I or ^{188}Re. Based on the critical role of the chemokine RANTES (regulated on activation, normal T-cell expressed and presumably secreted)/CCL5 secreted by MSCs in the course of tumor stroma recruitment, use of the RANTES/CCL5 promoter should allow tumor stroma-targeted expression of NIS after MSC-mediated delivery. Using a human hepatocellular cancer (HCC) xenograft mouse model (Huh7), we investigated distribution and tumor recruitment of RANTES-NIS-engineered MSCs after systemic injection by gamma camera imaging. ^{123}I-scintigraphy revealed active MSC recruitment and CCL5 promoter activation in the tumor stroma of Huh7 xenografts (6.5% ID/g ^{123}I, biological half-life: 3.7 hr, tumor-absorbed dose: 44.3 mGy/MBq). In comparison, 7% ID/g ^{188}Re was accumulated in tumors with a biological half-life of 4.1 hr (tumor-absorbed dose: 128.7 mGy/MBq). Administration of a therapeutic dose of ^{131}I or ^{188}Re (55.5 MBq) in RANTES-NIS-MSC-treated mice resulted in a significant delay in tumor growth and improved survival without significant differences between ^{131}I and ^{188}Re. These data demonstrate successful stromal targeting of NIS in HCC tumors by selective recruitment of NIS-expressing MSCs and by use of the RANTES/CCL5 promoter. The resulting tumor-selective radionuclide accumulation was high enough for a therapeutic effect of ^{131}I and ^{188}Re opening the exciting prospect of NIS-mediated radionuclide therapy of metastatic cancer using genetically engineered MSCs as gene delivery vehicles.

Introduction

Hepatocellular carcinoma (HCC) is the sixth most common malignancy and the third leading cause of cancer-related death worldwide (Parkin *et al.*, 2005). The only available, potentially curative treatment options, such as liver transplantation, surgical resection, or radiofrequency ablation, are reserved for patients with early-stage HCC. However, more than half of the patients with HCCs are diagnosed at an intermediate or advanced tumor stage with only limited, palliative treatment options, leading to a poor prognosis for these patients (Parkin *et al.*, 2005; Pinter *et al.*, 2012). Growing HCC requires an active tumor stroma with extensive vasculature with high endothelial cell turnover, numerous cancer-associated fibroblasts, inflammatory cells, and increased levels of cytokines and chemokines such as TNF-α, TGF-β, IL-6, IL-10, CCL2/MCP-1, CCL3, and RANTES (regulated on activation, normal T-cell expressed and presumably secreted)/CCL5 for effective tumor growth (Niess *et al.*, 2011; Braunersreuther *et al.*, 2012). The tumor stroma is therefore recognized as an important therapeutic target in the treatment of HCCs.

Mesenchymal stem cells (MSC) play a key role in the maintenance and regeneration of diverse tissues. In the course of tissue injury, or during chronic inflammation, MSCs contribute to tissue remodeling by their recruitment to sites of tissue injury (Aquino *et al.*, 2010). We, and others, have shown that MSCs are strongly recruited into the stroma

[1]Department of Internal Medicine II; [2]Clinical Biochemistry Group, Department of Medical Policlinic IV; [3]Department of Nuclear Medicine, Department of Pharmacy, Center of Drug Research; [4]Pharmaceutical Biotechnology; Ludwig-Maximilians-University, Munich 81377, Germany.

of many malignant tumors. It is thought that the growing tumor is seen by the body as a "chronic wound," and MSCs act as progenitor cells for components of the tumor stroma (Conrad *et al.*, 2007; Zischek *et al.*, 2009; Aquino *et al.*, 2010; Dwyer *et al.*, 2010; Conrad *et al.*, 2011; Knoop *et al.*, 2011; Niess *et al.*, 2011). The tropism of MSCs for tumors represents the basis for the paradigm of the "Trojan horse" approach. Due to their intrinsic tumor-homing capacity, MSCs are under development as cellular vehicles for the targeted delivery of therapeutic genes into the stroma of malignant tumors (Klopp *et al.*, 2007; Zischek *et al.*, 2009; Knoop *et al.*, 2011; Niess *et al.*, 2011).

Central issues that must be addressed with this therapeutic approach include the development of restricted transgene expression to spare potential damage to nontumor tissues, enhanced noninvasive *in vivo* imaging techniques that could be applied to patients, and the development of more potent therapy gene strategies.

Karnoub *et al.* (2007) recently demonstrated recruitment of MSCs into the tumor stroma of breast cancer, followed by their induced expression of the CC-chemokine RANTES/CCL5. CCL5 is a chemoattractant of monocytes, eosinophils, and activated CD4 T cells, which signals through the G protein-coupled receptors (GPCR) CCR1, CCR3, and CCR5 (Zlotnik and Yoshie, 2000). CCL5 expression is associated with increased tumor neovascularization, as well as enhanced cancer growth and metastasis by autocrine and paracrine activation of tumor cells and through the recruitment of stromal cell types to sites of primary tumor growth (Karnoub *et al.*, 2007).

Due to its expression in follicular cell-derived thyroid cancer cells, the sodium iodide symporter (NIS) provides the molecular basis for diagnostic and therapeutic application of radioiodine for the treatment of thyroid cancer patients. Cloning of *NIS* has therefore allowed the development of a new therapeutic strategy for the treatment of tumors without endogenous *NIS* expression based on targeted, tumor-selective *NIS* gene transfer followed by administration of ^{131}I or other radionuclides that are transported by NIS, such as ^{188}Re or ^{211}At (Spitzweg and Morris, 2002; Willhauck *et al.*, 2007, 2008a; Hingorani *et al.*, 2010). ^{188}Re is characterized by a shorter physical half-life and decay properties that are seen as superior to ^{131}I, and thus may provide a powerful tool to enhance the therapeutic efficacy of NIS-mediated radionuclide therapy, in particular because of its enhanced crossfire effect (max path length of up to 10.4 mm) (Willhauck *et al.*, 2007; Klutz *et al.*, 2011). Importantly, the use of NIS as a theranostic gene offers the possibility of direct noninvasive molecular scintigraphy and PET imaging allowing dosimetric calculations as a crucial prerequisite for the exact planning of therapy studies (Spitzweg and Morris, 2002; Dingli *et al.*, 2003; Groot-Wassink *et al.*, 2004; Willhauck *et al.*, 2007; Klutz *et al.*, 2011).

In our previous studies, human MSCs were stably transfected with a sodium iodide symporter (NIS)-expressing plasmid, where *NIS* was driven by the broadly expressed cytomegalovirus (CMV) promoter. Using *NIS* as reporter gene, active MSC recruitment into the tumor stroma of HCC xenografts was demonstrated after systemic injection. In addition, repetitive MSC injections followed by ^{131}I administration showed a significant reduction in tumor growth with an improved survival (Knoop *et al.*, 2011). Since MSCs are known to be recruited also in nontumor tissues such as spleen or skin, the use of the unspecific CMV promoter might be disadvantageous due to transgene expression in these nontarget organs with the risk of extratumoral toxicity. Therefore, in the current study, we have made use of the RANTES/CCL5 promoter to biologically target NIS transgene expression in engineered human MSCs to the stroma of HCC xenografts. In parallel, the accumulation and therapeutic efficacy of ^{131}I was examined in direct comparison to ^{188}Re in the context of systemic MSC-mediated NIS gene transfer.

Materials and Methods

Cell culture

Establishment and characterization of MSCs and cultivation of the human HCC cell line Huh7 (JCRB 0403) have been described previously (Knoop *et al.*, 2011).

Plasmid construct

The full-length NIS cDNA was removed from the pcDNA3 expression vector (kindly provided by Dr S.M. Jhiang, Ohio State University, Columbus, OH) by restriction digestion using XbaI and HindIII, agarose gel purified and ligated into the expression vector pcDNA3-CCL5Pro. CCL5Pro-NIS was removed and ligated in the pCMV/Bsd vector (Invitrogen/Life Technologies) using the restriction enzyme HindIII resulting in pCMV/Bsd-RaPro-hNIS. The sequence of the CCL5 promoter used −972 of the upstream region and the complete 5′ untranslated region (Nelson *et al.*, 1993). The vector included a CMV-controlled Bsr2 blasticidin resistance gene to select transfected cells at a blasticidin concentration of 5 μg/ml.

Mesenchymal stem cells

Wild-type MSCs stably transfected with pCMV/Bsd-RaPro-hNIS were established as described previously (Knoop *et al.*, 2011). The clone expressing the highest levels of NIS mRNA was subsequently referred to as RANTES-NIS-MSC and used for all further experiments. To prepare cells for injection into mice, cells were detached from culture flasks, washed three times with 1 × phosphate buffered saline (PBS) and resuspended in 1 × PBS at a concentration of 500,000 cells per 500 μl.

Establishment of Huh7 xenograft tumors

Huh7 xenograft tumors were established in female CD1 nu/nu mice (Charles River) as described previously (Knoop *et al.*, 2011). The experimental protocol was approved by the regional governmental commission for animals (Regierung von Oberbayern).

MSC application and radionuclide biodistribution analysis in vivo

Experiments were started when a tumor size of 3 to 5 mm was reached and following a 10-day pretreatment with L-T4 as described previously (Knoop *et al.*, 2011). The pretreatment schedule was based on a study by Di Cosmo *et al.* (2009) using a dose generally accepted as a supraphysiological LT-4 dose (10 μg L-T4/100 g body weight). The mice

used in our experiments weighed between 20–25 g, and therefore a dose of 2 μg L-T4/mice per day was chosen. Wild-type (WT)-MSCs or RANTES-NIS-MSCs were injected into the tail vein at a concentration of 5×10^5 cells/500 μl PBS. Two groups of mice were established with the following treatments: (a) three i.v. applications of RANTES-NIS-MSC in four-day intervals (n = 48) and (b) three i.v. applications of WT-MSC in four-day intervals (n = 9). As an additional control, in a subset of mice injected with RANTES-NIS-MSC (n = 18), the specific NIS inhibitor sodium-perchlorate ($NaClO_4$, 2 mg per mouse) was injected i.p. 30 min prior to radionuclide administration. Seventy-two hr after the last MSC application, 18.5 MBq ^{123}I or 111 MBq ^{188}Re ($^{188}ReO_4^-$ perrenhate) were injected i.p., and radionuclide biodistribution was assessed using a gamma camera equipped with UXHR collimator (Ecam) as described previously (Willhauck *et al.*, 2007, 2008a; Knoop *et al.*, 2011).

Biodistribution analysis of radionuclides was also performed *ex vivo* after mice were injected with RANTES-NIS-MSCs (n = 16) or WT-MSCs (n = 6), as described above, followed by i.p. injection of 18.5 MBq ^{123}I or 111 MBq ^{188}Re, respectively. As an additional control, a subset of RANTES-NIS-MSC-injected mice (n = 8) were pretreated with $NaClO_4$. Gamma counter analysis was performed as described previously (Knoop *et al.*, 2011).

NIS mRNA analysis by quantitative real-time PCR

Analysis of NIS mRNA expression by quantitative real-time polymerase chain reaction (qPCR) was performed as described previously (Klutz *et al.*, 2009; Knoop *et al.*, 2011).

Radionuclide therapy studies in vivo

Following a 10-day L-T4 pretreatment as described above, four groups of mice were established receiving 55.5 MBq ^{131}I (sodium iodide; GE Healthcare Buchler GmbH) or ^{188}Re ($^{188}ReO_4^-$ perrhenate; ITG GmbH) 48 hr after the final of three RANTES-NIS-MSC (RANTES-NIS-MSC + ^{131}I, n = 15; RANTES-NIS-MSC + ^{188}Re, n = 15) or WT-MSC (WT-MSC + ^{131}I, n = 15; WT-MSC + ^{188}Re, n = 15) applications in two-day-intervals (each 5×10^5 cells/500 μl PBS), respectively. This cycle was repeated once 24 hr after the last radionuclide application. Twenty-four hr later, one additional MSC (5×10^5 cells) injection was applied, followed by another radionuclide (55.5 MBq ^{131}I or ^{188}Re, respectively) injection 48 hr later. As a control group, mice were injected with RANTES-NIS-MSC (n = 15) followed by application of saline. Another control group received saline only (n = 15). The follow-up of mice, including tumor measurements, were performed as outlined previously (Knoop *et al.*, 2011).

Indirect immunofluorescence assay

Immunofluorescence staining of frozen sections was performed as described previously (Knoop *et al.*, 2011) using the following primary antibodies: hNIS (mouse monoclonal, provided by J.C. Morris, Division of Endocrinology, Mayo Clinic and Medical School, Rochester, MN); mouse RANTES/CCL5 (goat polyclonal, AF478, R&D Systems), SV40 large T-antigen (mouse monoclonal, Calbiochem/Merck), CD31 (rat monoclonal, Pharmingen/BD), or Ki67 (rabbit polyclonal, Abcam). Staining and evaluation of proliferation and vessel density were preformed as described previously (Knoop *et al.*, 2011).

Statistical methods

Statistical significance of *in vitro* experiments was tested using Student's t test. Statistical significance of *in vivo* experiments has been calculated using Man-Whitney U test.

Results

Radionuclide biodistribution studies after in vivo *NIS gene transfer*

Significant iodide accumulation was observed in 67% of Huh7 tumors following application of RANTES-NIS-MSCs (Fig. 1A). In contrast, after application of WT-MSCs no tumoral iodide accumulation was measured (Fig. 1C). Serial imaging revealed a tumoral uptake of approximately 6.5% ID/g ^{123}I after application of RANTES-NIS-MSCs, with a biological half-life of 3.7 hr (Fig. 1G). Considering a tumor mass of 1 g, and an effective half-life of 3.5 hr for ^{131}I, a tumor-absorbed dose of 44.3 ± 8.6 mGy/MBq ^{131}I was calculated. In comparison, approximately 7% ID/g ^{188}Re was concentrated in 67% of Huh7 tumors, with a biological half life of 4.1 hr (Fig. 1D and G). With an effective half life of 3.5 hr for ^{188}Re, a tumor-absorbed dose of 128.7 ± 28.2 mGy/MBq ^{188}Re was determined. Physiologic accumulation of radionuclides was also observed in thyroid gland and stomach, due to endogenous NIS expression, as well as in the bladder due to renal excretion of radionuclides (Fig. 1A, C, D, F). In a subset of mice injected with RANTES-NIS-MSCs, pretreatment with perchlorate ($NaClO_4$; 2 mg), 30 min prior to injection of the respective radionuclide, completely abolished radionuclide uptake in the tumor as well as in the thyroid gland and stomach, confirming that the observed radionuclide accumulation is indeed NIS-mediated (Fig. 1B and E). As expected, physiologic radionuclide accumulation in nontarget organs (thyroid gland, stomach, and bladder) was also seen after WT-MSC injection (Fig. 1C and F). As outlined above, in 1/3 of the animals no specific radionuclide accumulation after RANTES-NIS-MSCs injection was observed, however, by immunohistochemistry it was shown that MSCs were recruited into the tumor stroma to a lower extent (Supplementary Fig. 1; Supplementary Data available online at www.liebertonline.com/hum), resulting in a radionuclide accumulation that was obviously below the detection limit.

Analysis of NIS protein expression by indirect immunofluorescence

The distribution of MSCs in tumors and nontarget organs such as liver, kidney, and spleen was determined in more detail by immunofluorescence staining using NIS-, SV40 large T Ag- and RANTES/CCL5-specific antibodies. Hematoxylin and eosin (H&E stainings) of all organs or tumors are provided (Fig. 2D, H, L, P, T). Immortalization of MSCs via SV40 large T Ag provides a useful marker for the *ex vivo* detection of adoptively transferred MSCs. NIS-specific immunoreactivity based on RANTES/CCL5 promoter activity was detected throughout the tumor stroma, predominantly in the vicinity of blood vessels, which paralleled the localization of SV40 large T Ag and the distribution of RANTES/

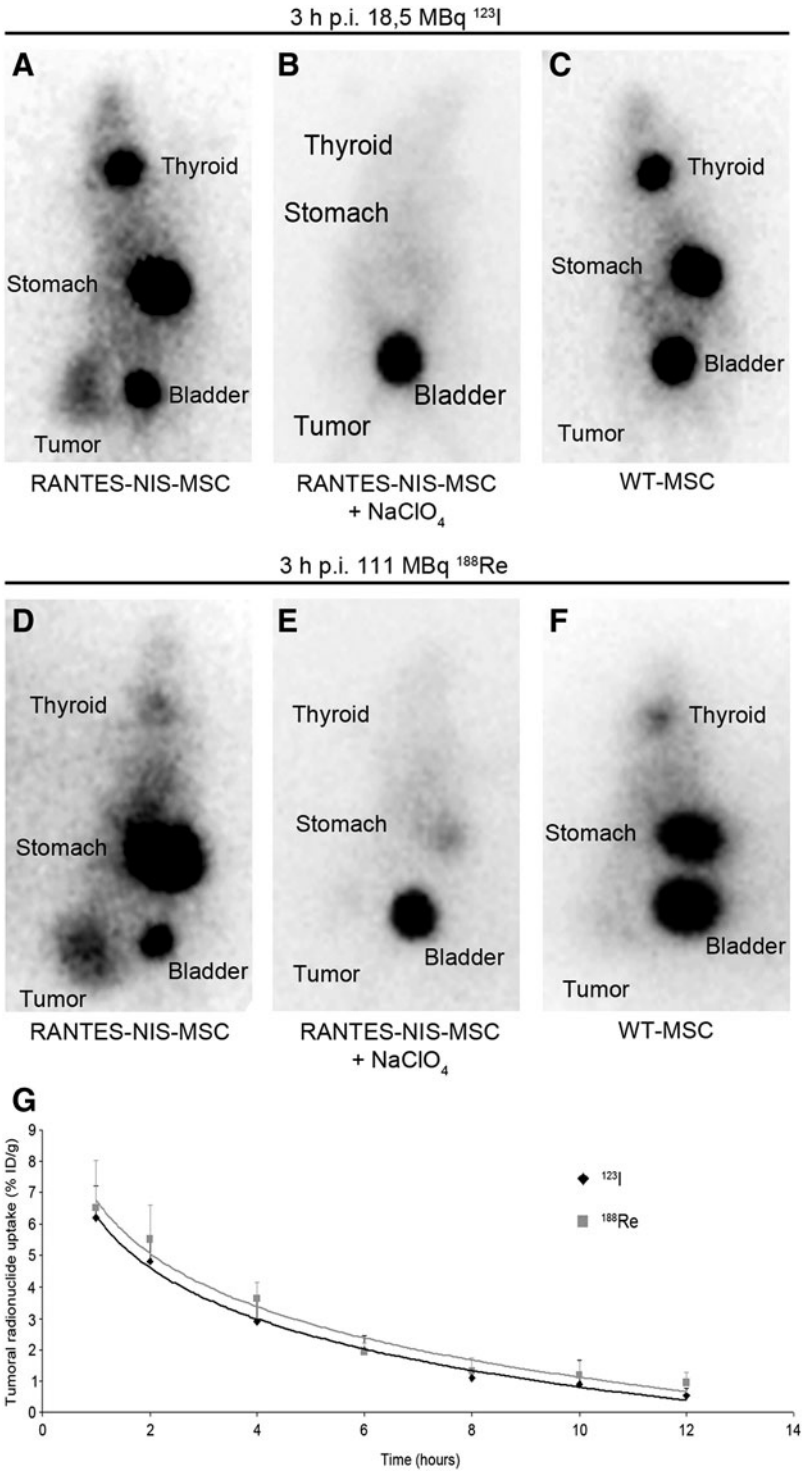

FIG. 1. Radionuclide biodistribution studies *in vivo*. Gamma-camera imaging of mice harboring Huh7 tumors after mesenchymal stem cell (MSC)-mediated sodium iodide symporter (NIS) gene delivery 3 hr following ^{123}I or ^{188}Re administration. After three intravenous i.v. applications of RANTES-NIS-MSCs significant tumor-specific iodide **(A)** and rhenium **(D)** accumulation was induced, which was completely abolished upon pretreatment with $NaClO_4$ **(B)** and **(E)**. In contrast, mice injected with wild-type (WT)-MSCs showed no tumoral iodide **(C)** or rhenium **(F)** uptake. Radionuclides were also accumulated physiologically in thyroid, stomach, and bladder. **(G)** Time course of ^{123}I and ^{188}Re accumulation in Huh7 tumors after three i.v. RANTES-NIS-MSC applications followed by injection of 18.5 MBq ^{123}I or 111 MBq ^{188}Re, respectively, as determined by serial scanning. Maximum tumoral radioiodine uptake was 6.5% ID/g tumor and 7% ID/g tumor for ^{188}Re, respectively. RANTES, regulated on activation, normal T-cell expressed and presumably secreted.

CCL5 expression (Fig. 2A–C). Liver and kidneys showed no detectable NIS, SV40 large T Ag, or RANTES/CCL5 immunoreactivity (Fig. 2E–G, I–K). In contrast, a high density of SV40 large T Ag–expressing cells was detected in the spleen after RANTES-NIS-MSC application (Fig. 2N), while no NIS- and RANTES/CCL5-specific immunofluorescence staining was observed (Fig. 2M and O), demonstrating restricted transgene expression. Injection of WT-MSCs resulted in SV40 large T Ag– and RANTES/CCL5-specific immunofluorescence staining in tumors (Fig. 2R and S), demonstrating active tumoral recruitment of MSCs after i.v. application. In contrast, no NIS-specific immunostaining was observed after WT-MSC gene transfer (Fig. 2Q).

Ex vivo *radionuclide biodistribution studies*

Significant levels of tumoral iodide and rhenium uptake were confirmed after application of RANTES-NIS-MSCs by

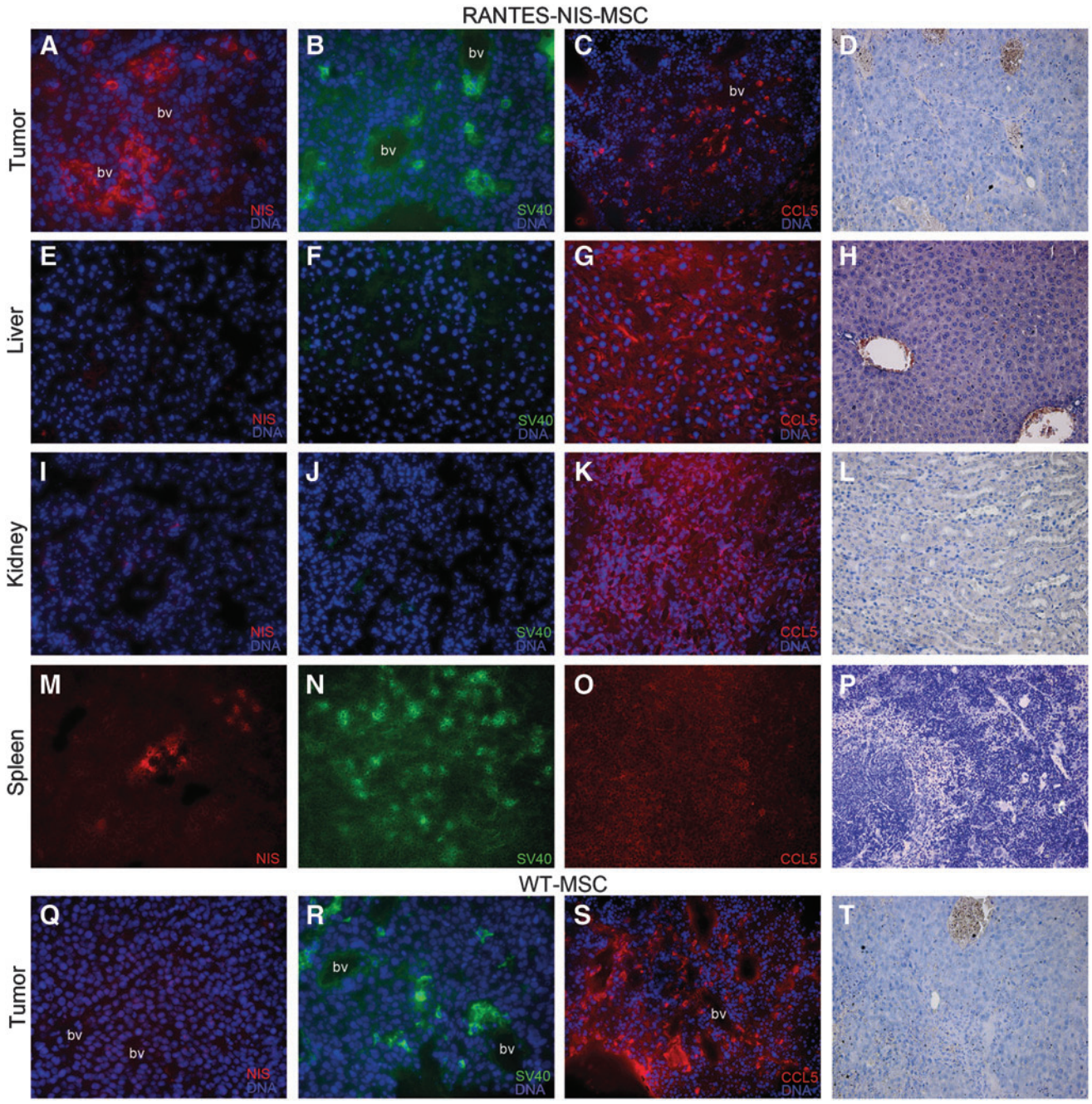

FIG. 2. Immunohistochemical staining of Huh7 tumors and nontarget organs after application of RANTES-NIS-MSCs or WT-MSCs. After application of RANTES-NIS-MSCs, Huh7 tumors revealed NIS-specific immunoreactivity throughout the tumor stroma **(A)** with a similar distribution of SV40 large T Ag- **(B)** and RANTES/CCL5-positive cells **(C)**. Other organs, like liver or kidney, showed no detectable NIS, SV40 large T Ag, or RANTES/CCL5 protein expression **(E–G; I–K)**. In contrast, strong accumulation of SV40 large T Ag-expressing cells was detected in the spleen of mice that were injected with RANTES-NIS-MSCs **(N)**, while no NIS- **(M)** or RANTES/CCL5-specific immunoreactivity **(O)** was detected. After application of WT-MSCs, no NIS-specific immunoreactivity was detected in Huh7 tumors **(Q)**, while strong cytoplasmatic SV40 large T Ag **(R)** and RANTES/CCL5 **(S)** staining was detected. Slides were counterstained with Hoechst nuclear stain. Hematoxylin and eosin (H&E) stainings of Huh7 tumors **(D)**, liver **(H)**, kidney **(L),** and spleen **(P)** after injection of RANTES-NIS-MSC and tumors of mice injected with WT-MSCs **(T)** are provided. Magnification: NIS, SV40 large T AG and H&E staining: ×200; RANTES/CCL5 staining: ×100. Bv, blood vessel.

ex vivo biodistribution studies revealing a radionuclide uptake of 3 – 3.5% ID/organ ^{123}I or ^{188}Re four hours after radionuclide injection. In nontarget organs (lung, liver, spleen, kidney) no specific radionuclide accumulation was detected. The competitive NIS inhibitor perchlorate significantly blocked radionuclide uptake in tumors of mice injected with RANTES-NIS-MSCs (Fig. 3). Significant radionuclide accumulation was also detected in tissues that physiologically express NIS (stomach, thyroid gland) and in the bladder due to renal elimination of radionuclides (Spitzweg *et al.*, 2001,

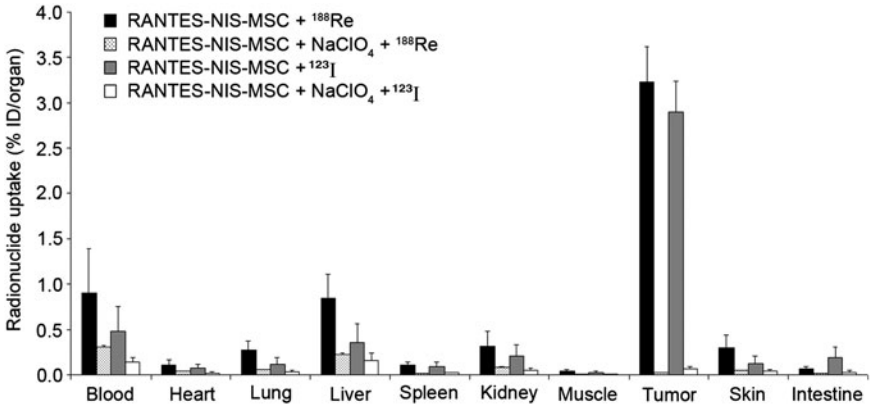

FIG. 3. Evaluation of radionuclide biodistribution *ex vivo* 4 hr following injection of 18.5 MBq ^{123}I or 111 MBq ^{188}Re. Tumors in RANTES-NIS-MSC-injected mice showed high perchlorate-sensitive radionuclide uptake activity (~3–3.5% ID/organ), while no significant radionuclide accumulation was measured in nontarget organs. Results are reported as percent of injected dose per organ ± SD.

2002). The thyroid gland and the stomach accumulated approximately 40% and 39% ID/organ, respectively, for ^{123}I and 15% ID/organ and 40% ID/organ, respectively, for ^{188}Re (data not shown). The effective half-life in the thyroid gland was approx. 38 hr for ^{131}I and only 6.5 hr for ^{188}Re. In this regard, it is important to outline that NIS expression is exclusively regulated by thyroid stimulating hormone (TSH) in the thyroid gland, which allows effective downregulation of radionuclide accumulation in the thyroid gland by thyroid hormone pretreatment as shown by Wapnir *et al.* (2004). Moreover, during prolonged anaesthesia for imaging purposes, gastric juices are pooled in the stomach, which results in significantly higher gastric radionuclide accumulation than routinely observed in humans. In the bladder, radionuclide accumulation and retention time can be minimized by stimulation of diuresis, thereby lowering the delivered dose and side effects to bladder and adjacent tissues.

NIS mRNA analysis by qPCR

mRNA was isolated from tumors and nontarget organs (liver, lung, kidney, and spleen) after systemic MSC injection and analyzed by qPCR using NIS-specific oligonucleotide primers. Systemic injection of RANTES-NIS-MSCs in tumor-bearing mice resulted in significantly increased levels of NIS mRNA in tumors, whereas no significant NIS mRNA expression was detected in nontarget organs (Fig. 4).

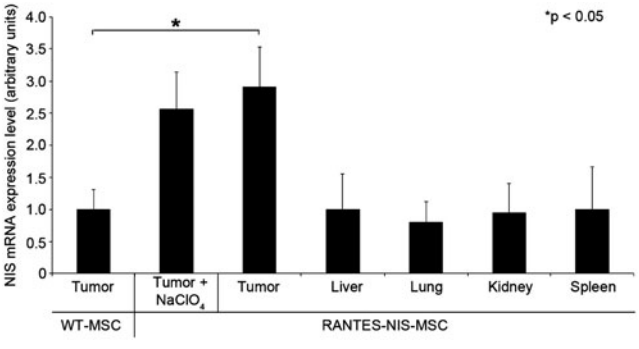

FIG. 4. Analysis of NIS mRNA expression in Huh7 tumors and nontarget organs by quantitative real-time polymerase chain reaction (qPCR). While only a low background level of NIS mRNA expression was detected in tumors injected with WT-MSCs, significant levels of NIS mRNA expression were induced in Huh7 tumors after three applications of RANTES-NIS-MSCs with or without $NaClO_4$ pretreatment. In nontarget organs like liver, lung, kidney, or spleen, no NIS mRNA expression was detected.

Radionuclide therapy studies in vivo *after MSC-mediated systemic NIS gene transfer*

The effect of therapeutic radionuclides (^{131}I and ^{188}Re) was then compared and contrasted in the context of RANTES-NIS-MSC treatment. Control mice treated with RANTES-NIS-MSCs followed by saline application, mice treated with WT-MSCs followed by application of ^{131}I or ^{188}Re, or mice treated with saline only showed an exponential tumor growth and had to be killed after 3–4 weeks (Fig. 5A). In contrast, RANTES-NIS-MSC and ^{131}I- or ^{188}Re-treated tumors showed a dramatic control of growth (day 24: $p = 0.02$ [NaCl] and $p = 0.05$ [WT-MSC]) that extended through the end of the experiment (nine weeks) (Fig. 5A) and that resulted in an improved survival (Fig. 5B). The application of ^{188}Re did not result in an obvious increase in therapeutic efficacy as compared with ^{131}I, but enhanced therapeutic effects would be difficult due to the dramatic effects of ^{131}I treatment in this experimental setting. No major adverse effects of radionuclide or MSC treatment were observed in terms of lethargy or respiratory failure.

At the end of the observation period, mice were sacrificed and tumors dissected, followed by H&E staining (Fig. 6F and G) and immunofluorescence staining using a Ki67-specific antibody (green, labeling proliferating cells) and a CD31-specific antibody (red, labeling blood vessels). Striking differences were observed between mice treated with WT-MSC (Fig. 6A and B) or mice treated with saline (Fig. 6C) as compared to mice treated with RANTES-NIS-MSC followed by application of ^{188}Re or ^{131}I (Fig. 6D and E). Tumors of mice injected with RANTES-NIS-MSC followed by NaCl showed a Ki67-index of approximately 62 ± 8% and a mean vessel density of 4.25 ± 0.7% (Fig. 6H and I), whereas tumors treated with RANTES-NIS-MSC and ^{188}Re or ^{131}I showed significantly reduced levels of intratumoral proliferation index (20.3 ± 5%) and blood vessel density (1 ± 0.2%) (Fig. 6H and I).

Discussion

Several research groups including our own have demonstrated that mesenchymal stem cells (MSCs) are actively recruited into growing tumor stroma where they play a major

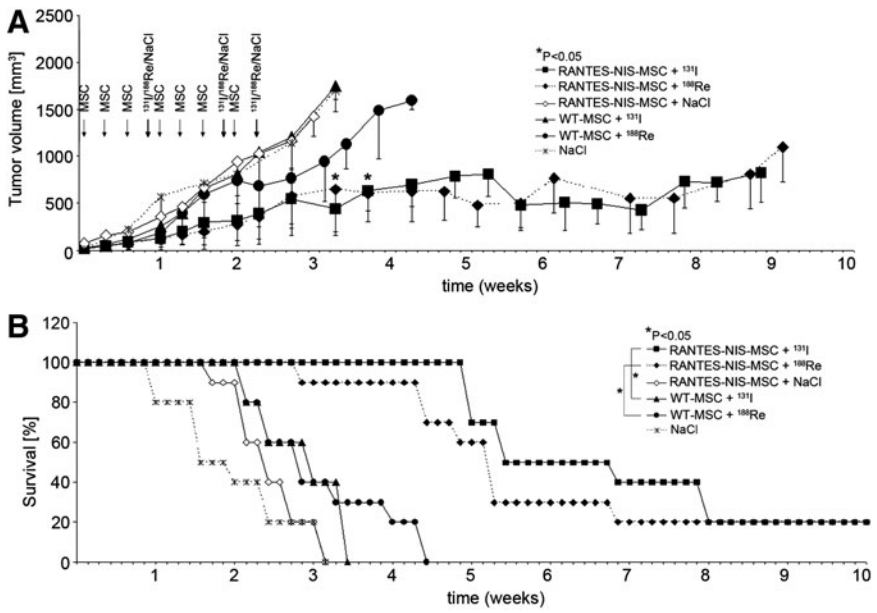

FIG. 5. Radionuclide therapy studies *in vivo* after MSC-mediated systemic NIS gene transfer. Four groups of mice were established receiving 55.5 MBq ^{131}I or ^{188}Re 48 hr after the final of three RANTES-NIS-MSC or WT-MSC applications in two-day-intervals. This cycle was repeated once 24 hr after the last radionuclide application. Twenty-four hours after these two treatment cycles, one additional MSC injection was administered followed by a third ^{131}I or ^{188}Re (55.5 MBq) injection 48 hr later. ^{131}I and ^{188}Re therapy after RANTES-NIS-MSC application resulted in a significant delay in tumor growth as compared with the control groups, which were injected with WT-MSCs followed by ^{131}I or ^{188}Re or with RANTES-NIS-MSCs followed by saline or with saline only ($p < 0.05$) **(Á)**. The significantly reduced tumor growth was associated with markedly improved survival (Kaplan-Meier-Plot, $p < 0.05$) **(B)**.

role in forming the tumor's fibrovascular network (Karnoub *et al.*, 2007; Zischek *et al.*, 2009; Knoop *et al.*, 2011; Niess *et al.*, 2011). MSC recruitment to tumor stroma is thought to be driven by high local concentrations of inflammatory chemokines and growth factors such as MCP-1/CCL2, IL-8/CXCL8, RANTES/CCL5, and SDF-1α/CXCL12 among others (Karnoub *et al.*, 2007; Spaeth *et al.*, 2008). Within the tumor stroma, MSCs can differentiate into carcinoma-associated fibroblasts or pericyte-like cells where they contribute to tumor growth through secretion of inflammatory and pro-angiogenic growth factors like VEGF, PDGF, SDF-1α/CXCL12, EGF, IGF, IL-6, and RANTES/CCL5 (Spaeth *et al.*, 2009). This tropism of MSCs for tumor environments makes them uniquely suited as tumor stroma–selective gene delivery vehicles. In models of pancreatic, breast, and liver cancer, we have applied MSCs transduced with herpes simplex virus type 1 thymidine kinase (HSV-Tk) and demonstrated active tumor stroma–selective recruitment of MSCs that significantly reduced tumor growth and metastasizing potential after treatment with ganciclovir (Zischek *et al.*, 2009; Niess *et al.*, 2011).

MSCs have been used to deliver a diverse array of agents, including interferon-β, cytosine deaminase, tumor necrosis factor–related apoptosis-inducing ligand, the immunostimulatory chemokine CX3CL1, and oncolytic viruses. These approaches have generally yielded positive antitumor effects (Spaeth *et al.*, 2008; Braunersreuther *et al.*, 2012). While effective, we sought to evaluate a potentially more flexible and potent therapy gene approach using the sodium iodide symporter (NIS). In a previous study using a liver cancer mouse model, MSCs were transfected with NIS under the control of the broadly unspecific CMV promoter. The engineered cells were actively recruited to the tumor and induced a significant antitumor effect after application of ^{131}I (Knoop *et al.*, 2011). A similar approach was subsequently confirmed in a breast cancer model by Dwyer *et al.* (2011).

With its flexibility regarding diagnostics, imaging, and potent therapeutic actions, the NIS gene represents an important new dimension in MSC-mediated tumor therapy. Because of the potential side effects of MSC recruitment to nontumor tissues, we examined the potential linkage of restricted tissue expression delivered through the use of the RANTES/CCL5 promoter to NIS-mediated MSC therapy in a model of HCC.

Upregulation of RANTES/CCL5 by MSCs in tumor stroma is associated with their differentiation into cancer-associated fibroblasts. In a murine model of breast cancer, MSCs were shown to increase the number of lung metastases. These effects were mediated in part by the RANTES/CCL5 produced by the MSCs in the presence of breast cancer cells that acted in a paracrine fashion on cancer cells to enhance their motility, invasion, and metastasis (Karnoub *et al.*, 2007). Pinilla *et al.* (2009) demonstrated that MSCs derived from human adipose tissue (hASCs) produce RANTES/CCL5 in coculture with breast cancer cells or in breast cancer cell conditioned medium, thereby increasing invasion of cancer cells, and conclude that RANTES/CCL5 plays a crucial role for tumor invasion in the interplay of tissue resident stem cells from fat tissue and breast cancer cells.

In our study, human MSCs were engineered to express NIS under control of the RANTES/CCL5 promoter to more specifically target NIS expression to the tumor stroma and reduce potential side effects linked to MSC recruitment to nontumor tissues. Initial demonstration of tumor stroma–selective RANTES/CCL5 promoter-driven expression of reporter or therapy genes in engineered MSCs was provided by our own work (Zischek *et al.*, 2009), where murine MSCs stably transfected with either reporter genes (red fluorescent protein [RFP], enhanced green fluorescent protein [eGFP]), or a therapy gene (HSV-Tk) driven by the RANTES/CCL5 promoter was used to evaluate the dynamics of expression in mice carrying orthotopic, syngeneic pancreatic tumors (Zischek *et al.*, 2009). Application of ganciclovir in these animals resulted in a significant reduction in primary tumor growth, as well as reduced incidence of metastases (Zischek *et al.*, 2009). The CCL5-based transgenic approach was later

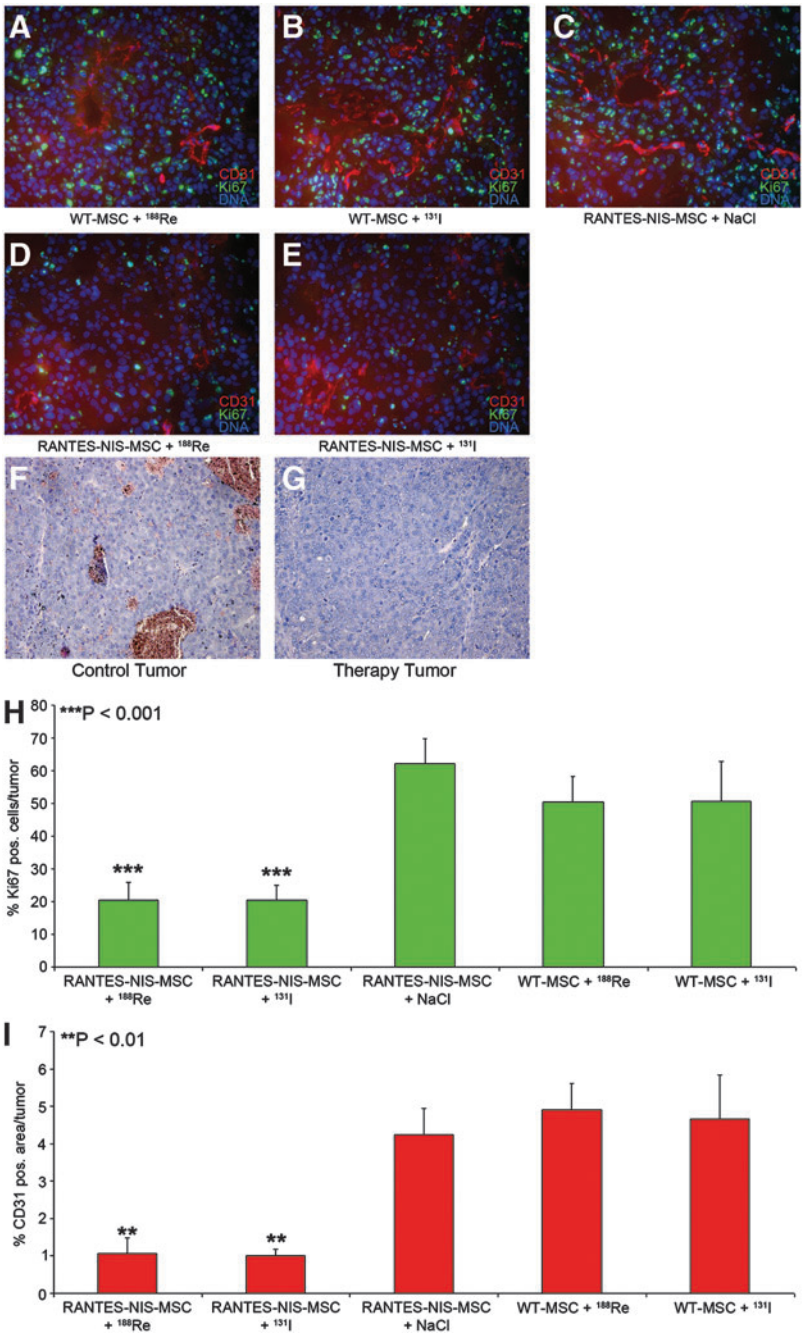

FIG. 6. Immunofluorescence analyses of radionuclide therapy studies. Immunofluorescence analysis of tumors using a Ki67-specific antibody (green, labeling proliferating cells) and an antibody against CD31 (red, labeling blood vessels). As compared to control tumors **(A–C)**, RANTES-NIS-MSC and ^{188}Re- or ^{131}I-treated tumors showed visible differences in tumor cell proliferation and blood vessel density **(D, E)**. Quantification of blood vessel density and tumor cell proliferation showed significantly reduced tumor cell proliferation (20.3 ± 5%) **(H)** and blood vessel density (1 ± 0.2%) **(I)** after systemic RANTES-NIS-MSC application in ^{188}Re- or ^{131}I-treated tumors as compared to control tumors (Ki67: 62 ± 8%, $p < 0.001$; CD31: 4.25 ± 0.7%, $p < 0.01$) **(H, I)**. Slides were counterstained with Hoechst nuclear stain. H&E stainings of control and treated tumors **(F, G)**. Magnification ×200.

directly compared to a Tie2-tumor angiogenesis–targeting approach in an orthotopic HCC xenograft model (Niess *et al.*, 2011). While both methods showed positive results, the results suggested a better outcome when the RANTES/CCL5 promoter was used to drive therapeutic transgenes in engineered MSC (Zischek *et al.*, 2009; Niess *et al.*, 2011).

In contrast to our experiments, most of the previously published studies analyzed MSC biodistribution and tumor-specific recruitment by *ex vivo* analysis of reporter gene expression. However, using NIS as a reporter gene allows efficient noninvasive imaging of transgene expression by ^{99m}Tc-scintigraphy, ^{123}I-scintigraphy or SPECT, and ^{124}I-PET imaging, as demonstrated in our study where tumor homing and engraftment of MSCs was noninvasively demonstrated by routine ^{123}I- or ^{188}Re-scintigraphy. This would allow an important new dimension in future patient studies, as exact planning of clinical gene therapy trials requires a thorough understanding of MSC biodistribution as well as level, duration, and distribution of transgene expression. Feasibility and efficacy of the NIS gene therapy approach using NIS as a theranostic gene has been shown in several former studies by different research groups including our own (Dwyer *et al.*, 2005a, 2005b; Herve *et al.*, 2008; Kakinuma *et al.*, 2003; Klutz *et al.*, 2009; Li *et al.*, 2010; Peerlinck *et al.*, 2009; Scholz *et al.*, 2005; Spitzweg *et al.*, 1999, 2000, 2001, 2007; Willhauck *et al.*, 2007, 2008a, 2008b, 2008c).

Following systemic application of RANTES-NIS-MSCs, 67% of implanted HCC tumors showed a tumor-specific ^{123}I

and ^{188}Re accumulation as shown by gamma camera imaging with a radionuclide accumulation of approximately 6–7% ID/g and a biological half-life of 3.7 hr, which is comparable to the data we had obtained in our previous study using the CMV promoter to drive NIS expression in MSCs (7–9% ID/g, biological half-life 4 hr) (Knoop *et al.*, 2011). Perchlorate injection prior to radionuclide application and the use of control MSCs confirmed NIS-specific radionuclide accumulation. The *in vivo* imaging data were confirmed by *ex vivo* biodistribution and immunofluorescence analysis, which demonstrated tumor stroma–specific accumulation of MSCs in addition to RANTES/CCL5 promoter activation as shown by immunohistochemical staining. In contrast, nontarget organs like liver or kidney showed no NIS, SV40 large T-Ag, or RANTES/CCL5 expression. Immunofluorescence analysis did reveal an accumulation of MSCs in the spleen, however, these cells did not show NIS-specific immunoreactivity. The presence of MSCs in the spleen may result either from direct recruitment of the cells (via CCR7) (Von Luttichau *et al.*, 2005) or from filtration of the exogenously applied MSCs from the peripheral circulation. Importantly, the lack of RANTES/CCL5 promoter-driven transgene expression demonstrates enhanced selectivity of the approach.

After three cycles of repetitive RANTES-NIS-MSC injection followed by the application of ^{131}I or ^{188}Re, an effective control of tumor growth was seen. This was associated with a dramatically improved survival of tumor-bearing animals to the end of the nine-week experiment. By contrast, control animals showed a maximum survival of 4 weeks. These results show a significant improvement over those we previously reported using the CMV promoter to drive NIS expression in the same model system where the mice lived 7 weeks after NIS-mediated radioiodine therapy (Knoop *et al.*, 2011).

In the current study, we also examined the potential use of ^{188}Re as an alternative therapeutic radionuclide to ^{131}I. ^{188}Re is also transported by NIS, but in contrast to ^{131}I, offers the possibility of higher energy deposition in the tumor in a shorter period of time due to its shorter physical half-life and higher energy. Another advantage is that ^{188}Re is less harmful to the thyroid, which is primarily caused by the lack of ^{188}Re organification and therefore significantly shorter effective half-life of ^{188}Re in the thyroid gland, thereby not only reducing radiation damage to the thyroid gland but also increasing tumoral ^{188}Re uptake by the elimination of the thyroid "sink" effect (Dadachova *et al.*, 2002). In consideration of the scattered MSC biodistribution in the tumor stroma, an enhanced therapeutic effect of ^{188}Re based on an increase in crossfire effect, due to the longer path length, was expected. In a breast cancer mouse model, Dadachova and colleagues showed a radiation dose 4.5 times higher for ^{188}Re than for ^{131}I, resulting in an improved therapeutic efficacy in mice (Dadachova *et al.*, 2005). Similarly, in one of our previous studies we have convincingly demonstrated the superior therapeutic effect of ^{188}Re as compared to ^{131}I in a prostate cancer xenograft mouse model based on a 4.7-fold higher tumor-absorbed dose after application of ^{188}Re as compared to ^{131}I (Willhauck *et al.*, 2007). In the current study, however, therapeutic efficacy of ^{188}Re compared to ^{131}I was similar in direct comparison, although, the tumor-absorbed dose for ^{188}Re was calculated to be three times higher than for ^{131}I (128.7 mGy/MBq vs. 44.3 mGy/MBq). Based on the survival curve obtained for both radionuclides, it is possible that a maximal therapeutic effect was already achieved with ^{131}I treatment. A more detailed titration of MSC and radionuclide application in future studies may allow a more precise contrasting of the therapeutic consequences of ^{188}Re vs. ^{131}I.

In addition, since dosimetric calculations are optimized for a homogenous tumoral radionuclide uptake and standard dosimetry models, not taking into account microdosimetry aspects, calculation of tumor-absorbed doses after MSC-mediated NIS gene transfer might be inaccurate due to inhomogeneous NIS expression and therefore inhomogenous radionuclide accumulation in the tumor stroma.

The mechanism underlying RANTES/CCL5 induction by MSC in tumor milieus is not well understood. Osteopontin (OPN), a secreted phosphoprotein that signals through $\alpha_v\beta_3$ integrin and CD44 (Denhardt *et al.*, 1995; McAllister *et al.*, 2008; Mi *et al.*, 2011) has been shown to induce expression of RANTES/CCL5 in MSCs (Mi *et al.*, 2011). EGFR and insulin-like growth factor 1 (IGF-1) signaling have also been linked to RANTES/CCL5 upregulation by MSCs (Mascia *et al.*, 2003; Karar and Maity, 2009). A better understanding of this biology may allow the reengineering of the RANTES/CCL5 promoter to optimize tumor specificity and reduce potential expression in other tissues (Grone *et al.*, 1999; Edelmann *et al.*, 2011).

Taken together, our data demonstrate high tumor selectivity of MSC recruitment and improved NIS expression driven by the RANTES/CCL5 promoter after systemic MSC application in an HCC xenograft model. The resulting biologically targeted, tumor-selective radionuclide accumulation was high enough for a therapeutic effect of ^{131}I and ^{188}Re opening the exciting prospect of NIS-mediated radionuclide therapy of metastatic cancer using engineered MSCs as gene delivery vehicles.

Acknowledgments

We are grateful to J.C. Morris, Division of Endocrinology, Mayo Clinic and Medical School, Rochester, Minnesota, for providing the NIS-specific antibody, as well as to S.M. Jhiang, Ohio State University, Columbus, Ohio, for supplying the full-length human NIS cDNA. We also thank W. Münzing, Julia Schlichtiger, and Heidrun Zankl, Department of Nuclear Medicine, Ludwig-Maximilians-University, Munich, Germany, for their assistance with the imaging and therapy studies. This study was supported by grant SFB 824 (Sonderforschungsbereich 824) from the Deutsche Forschungsgemeinschaft, Bonn, Germany, to C. Spitzweg and by a grant from the Wilhelm-Sander-Stiftung (2008.037.1) to C. Spitzweg and P.J. Nelson.

Author Disclosure Statement

No competing financial interests exist.

References

Aquino, J.B., Bolontrade, M.F., Garcia, M.G., *et al.* (2010). Mesenchymal stem cells as therapeutic tools and gene carriers in liver fibrosis and hepatocellular carcinoma. Gene Ther. 17, 692–708.

Braunersreuther, V., Viviani, G.L., Mach, F., and Montecucco, F. (2012). Role of cytokines and chemokines in non-alcoholic fatty liver disease. World J Gastroenterol. 18, 727–735.

Conrad, C., Gupta, R., Mohan, H., *et al.* (2007). Genetically engineered stem cells for therapeutic gene delivery. Curr Gene Ther. 7, 249–260.

Conrad, C., Huesemann, Y., Niess, H., *et al.* (2011). Linking Transgene Expression of Engineerd Mesenchymal Stem Cells and Angiopoietin-1-induced Differentiation to Target Cancer Angiogenesis. Ann Surg. 253, 566–571.

Dadachova, E., Bouzahzah, B., Zuckier, L.S., and Pestell, R.G. (2002). Rhenium-188 as an alternative to iodine-131 for treatment of breast tumors expressing the sodium/iodide symporter (NIS). Nucl Med Biol. 29, 13–18.

Dadachova, E., Nguyen, A., Lin, E.Y., *et al.* (2005). Treatment with rhenium-188-perrhenate and iodine-131 of NIS-expressing mammary cancer in a mouse model remarkably inhibited tumor growth. Nucl Med Biol. 32, 695–700.

Denhardt, D.T., Lopez, C.A., Rollo, E.E., *et al.* (1995). Osteopontin-induced modifications of cellular functions. Ann N Y Acad Sci. 760, 127–142.

Di Cosmo, C., Liao, X.H., Dumitrescu, A.M., *et al.* (2009). A thyroid hormone analog with reduced dependence on the monocarboxylate transporter 8 for tissue transport. Endocrinology 150, 4450–4458.

Dingli, D., Russell, S.J., and Morris, J.C. (2003). In vivo imaging and tumor therapy with the sodium iodide symporter. J Cell Biochem. 90, 1079–1086.

Dwyer, R.M., Bergert, E.R., O'Connor M, K., *et al.* (2005a). In vivo radioiodide imaging and treatment of breast cancer xenografts after MUC1-driven expression of the sodium iodide symporter. Clin Cancer Res. 11, 1483–1489.

Dwyer, R.M., Schatz, S.M., Bergert, E.R., *et al.* (2005b). A preclinical large animal model of adenovirus-mediated expression of the sodium-iodide symporter for radioiodide imaging and therapy of locally recurrent prostate cancer. Mol Ther. 12, 835–841.

Dwyer, R.M., Khan, S., Barry, F.P., *et al.* (2010). Advances in mesenchymal stem cell-mediated gene therapy for cancer. Stem Cell Res Ther. 1, 25.

Dwyer, R.M., Ryan, J., Havelin, R.J., *et al.* (2011). Mesenchymal Stem Cell-mediated delivery of the sodium iodide symporter supports radionuclide imaging and treatment of breast cancer. Stem Cells 29, 1149–1157.

Edelmann, S.L., Nelson, P.J., and Brocker, T. (2011). Comparative promoter analysis in vivo: identification of a dendritic cell-specific promoter module. Blood 118, e40–e49.

Grone, H.J., Weber, C., Weber, K.S., *et al.* (1999). Met-RANTES reduces vascular and tubular damage during acute renal transplant rejection: blocking monocyte arrest and recruitment. FASEB J. 13, 1371–1383.

Groot-Wassink, T., Aboagye, E.O., Wang, Y., *et al.* (2004). Quantitative imaging of Na/I symporter transgene expression using positron emission tomography in the living animal. Mol. Therapy 9, 436–442.

Herve, J., Cunha, A.S., Liu, B., *et al.* (2008). Internal radiotherapy of liver cancer with rat hepatocarcinoma-intestine-pancreas gene as a liver tumor-specific promoter. Hum Gene Ther. 19, 915–926.

Hingorani, M., Spitzweg, C., Vassaux, G., *et al.* (2010). The biology of the sodium iodide symporter and its potential for targeted gene delivery. Curr. Cancer Drug Targets 10, 242–267.

Kakinuma, H., Bergert, E.R., Spitzweg, C., *et al.* (2003). Probasin promoter (ARR(2)PB)-driven, prostate-specific expression of the human sodium iodide symporter (h-NIS) for targeted radioiodine therapy of prostate cancer. Cancer Res. 63, 7840–7844.

Karar, J., and Maity, A. (2009). Modulating the tumor microenvironment to increase radiation responsiveness. Cancer Biol Ther. 8, 1994–2001.

Karnoub, A.E., Dash, A.B., Vo, A.P., *et al.* (2007). Mesenchymal stem cells within tumour stroma promote breast cancer metastasis. Nature 449, 557–563.

Klopp, A.H., Spaeth, E.L., Dembinski, J.L., *et al.* (2007). Tumor irradiation increases the recruitment of circulating mesenchymal stem cells into the tumor microenvironment. Cancer Res. 67, 11687–11695.

Klutz, K., Russ, V., Willhauck, M.J., *et al.* (2009). Targeted radioiodine therapy of neuroblastoma tumors following systemic nonviral delivery of the sodium iodide symporter gene. Clin Cancer Res. 15, 6079–6086.

Klutz, K., Willhauck, M.J., Wunderlich, N., *et al.* (2011). Sodium iodide symporter (NIS)-mediated radionuclide ((131)I, (188)Re) therapy of liver cancer after transcriptionally targeted intratumoral in vivo NIS gene delivery. Hum Gene Ther. 22, 1403–1412.

Knoop, K., Kolokythas, M., Klutz, K., *et al.* (2011). Image-guided, tumor stroma-targeted 131I therapy of hepatocellular cancer after systemic mesenchymal stem cell-mediated NIS gene delivery. Mol Ther. 19, 1704–1713.

Li, H., Peng, K.W., Dingli, D., *et al.* (2010). Oncolytic measles viruses encoding interferon beta and the thyroidal sodium iodide symporter gene for mesothelioma virotherapy. Cancer Gene Ther. 17, 550–558.

Mascia, F., Mariani, V., Girolomoni, G., and Pastore, S. (2003). Blockade of the EGF receptor induces a deranged chemokine expression in keratinocytes leading to enhanced skin inflammation. Am. J. Pathol. 163, 303–312.

McAllister, S.S., Gifford, A.M., Greiner, A.L., *et al.* (2008). Systemic endocrine instigation of indolent tumor growth requires osteopontin. Cell 133, 994–1005.

Mi, Z., Bhattacharya, S.D., Kim, V.M., *et al.* (2011). Osteopontin promotes CCL5-mesenchymal stromal cell-mediated breast cancer metastasis. Carcinogenesis 32, 477–487.

Nelson, P.J., Kim, H.T., Manning, W.C., *et al.* (1993). Genomic organization and transcriptional regulation of the RANTES chemokine gene. J Immunol. 151, 2601–2612.

Niess, H., Bao, Q., Conrad, C., *et al.* (2011). Selective targeting of genetically engineered mesenchymal stem cells to tumor stroma microenvironments using tissue-specific suicide gene expression suppresses growth of hepatocellular carcinoma. Ann Surg. 254, 767–774.

Parkin, D.M., Bray, F., Ferlay, J., and Pisani, P. (2005). Global cancer statistics, 2002. CA Cancer J. Clin. 55, 74–108.

Peerlinck, I., Merron, A., Baril, P., *et al.* (2009). Targeted radionuclide therapy using a Wnt-targeted replicating adenovirus encoding the Na/I symporter. Clin Cancer Res. 15, 6595–6601.

Pinilla, S., Alt, E., Abdul Khalek, F.J., *et al.* (2009). Tissue resident stem cells produce CCL5 under the influence of cancer cells and thereby promote breast cancer cell invasion. Cancer Lett. 284, 80–85.

Pinter, M., Hucke, F., Graziadei, I., *et al.* (2012). Advanced-Stage Hepatocellular Carcinoma: Transarterial Chemoembolization versus Sorafenib. Radiology 263, 590–599.

Scholz, I.V., Cengic, N., Baker, C.H., *et al.* (2005). Radioiodine therapy of colon cancer following tissue-specific sodium iodide symporter gene transfer. Gene Ther. 12, 272–280.

Spaeth, E., Klopp, A., Dembinski, J., *et al.* (2008). Inflammation and tumor microenvironments: defining the migratory itinerary of mesenchymal stem cells. Gene Ther. 15, 730–738.

Spaeth, E.L., Dembinski, J.L., Sasser, A.K., *et al.* (2009). Mesenchymal stem cell transition to tumor-associated fibroblasts contributes to fibrovascular network expansion and tumor progression. PLoS One 4, e4992.

Spitzweg, C., Zhang, S., Bergert, E.R., *et al.* (1999). Prostate-specific antigen (PSA) promoter-driven androgen-inducible expression of sodium iodide symporter in prostate cancer cell lines. Cancer Res. 59, 2136–2141.

Spitzweg, C., O'Connor, M.K., Bergert, E.R., *et al.* (2000). Treatment of prostate cancer by radioiodine therapy after tissue-specific expression of the sodium iodide symporter. Cancer Res 60, 6526–6530.

Spitzweg, C., Dietz, A.B., O'Connor, M.K., *et al.* (2001). In vivo sodium iodide symporter gene therapy of prostate cancer. Gene Ther. 8, 1524–1531.

Spitzweg, C., and Morris, J.C. (2002). The sodium iodide symporter: its pathophysiological and therapeutic implications. Clin. Endocrinol. (Oxf) 57, 559–574.

Spitzweg, C., Baker, C.H., Bergert, E.R., *et al.* (2007). Image-guided radioiodide therapy of medullary thyroid cancer after carcinoembryonic antigen promoter-targeted sodium iodide symporter gene expression. Hum. Gene Ther. 18, 916–924.

Van Sande, J., Massart, C., Beauwens, R., *et al.* (2003). Anion selectivity by the sodium iodide symporter. Endocrinology 144, 247–252.

Von Luttichau, I., Notohamiprodjo, M., Wechselberger, A., *et al.* (2005). Human adult CD34- progenitor cells functionally express the chemokine receptors CCR1, CCR4, CCR7, CXCR5, and CCR10 but not CXCR4. Stem Cells Dev. 14, 329–336.

Wapnir, I.L., Goris, M., Yudd, A., *et al.* (2004). The Na+/I-symporter mediates iodide uptake in breast cancer metastases and can be selectively down-regulated in the thyroid. Clin Cancer Res. 10, 4294–4302.

Willhauck, M.J., Sharif-Samani, B.R., Gildehaus, F.J., *et al.* (2007). Application of 188Re as an Alternative Radionuclide for Treatment of Prostate Cancer after Tumor-Specific Sodium Iodide Symporter Gene Expression. J. Clin. Endocrinol Metab. 92, 4451–4458.

Willhauck, M.J., Samani, B.R., Wolf, I., *et al.* (2008a). The potential of 211Astatine for NIS-mediated radionuclide therapy in prostate cancer. Eur. J. Nucl. Med. Mol. Imaging 35, 1272–1281.

Willhauck, M.J., Sharif-Samani, B., Senekowitsch-Schmidtke, R., *et al.* (2008b). Functional sodium iodide symporter expression in breast cancer xenografts in vivo after systemic treatment with retinoic acid and dexamethasone. Breast Cancer Res. Treat. 109, 263–272.

Willhauck, M.J., Sharif Samani, B.R., Klutz, K., *et al.* (2008c). Alpha-fetoprotein promoter-targeted sodium iodide symporter gene therapy of hepatocellular carcinoma. Gene Ther. 15, 214–223.

Zischek, C., Niess, H., Ischenko, I., *et al.* (2009). Targeting tumor stroma using engineered mesenchymal stem cells reduces the growth of pancreatic carcinoma. Ann. Surg. 250, 747–753.

Zlotnik, A., and Yoshie, O. (2000). Chemokines: a new classification system and their role in immunity. Immunity 12, 121–127.

Address correspondence to:
Dr. Christine Spitzweg
Department of Internal Medicine II
University Hospital of Munich
Marchioninistrasse 15
81377 Munich
Germany

E-mail: christine.spitzweg@med.uni-muenchen.de

Received for publication May 24, 2012;
accepted after revision February 11, 2013.

Published online: February 12, 2013.